

Robust nuclear spin entanglement via dipolar interactions in polar molecules

Timur V. Tscherbul¹ Jun Ye², and Ana Maria Rey²

¹Department of Physics, University of Nevada, Reno, Nevada, 89557, USA

²JILA, National Institute of Standards and Technology, and Department of Physics, University of Colorado, Boulder, Colorado, 80309, USA

(Dated: May 3, 2022)

We propose a general protocol for on-demand generation of robust entangled states of nuclear and/or electron spins of ultracold $^1\Sigma$ and $^2\Sigma$ polar molecules using electric dipolar interactions. By encoding a spin-1/2 degree of freedom in a combined set of spin and rotational molecular levels, we theoretically demonstrate the emergence of effective spin-spin interactions of the Ising and XXZ forms, enabled by efficient magnetic control over electric dipolar interactions. We show how to use these interactions to create long-lived cluster and squeezed spin states.

Ultracold polar molecules hold great promise for quantum simulation, metrology and information processing because they feature strong electric dipolar (ED) interactions that are both long range, anisotropic, and, more importantly, tunable [1–16]. A necessary condition towards their use for these goals is the capability to take advantage of their intrinsic ED interactions to create highly entangled and long-lived molecular states that are robust to environmental decoherence, such as spin-squeezed states for enhanced sensing [17–19], or cluster states for measurement-based quantum computation [20–25].

Up to date, rotational states of simple bialkali molecules such as KRb have been proposed as the primary workhorse and a natural degree of freedom to encode a qubit [1–12]. This is because the long-lived rotational states can be directly coupled by long-range ED interactions and manipulated by microwave (mw) fields [26, 27]. Nevertheless, rotational states feature important limitations which have hindered their use for entanglement generation: (1) ultracold molecules prepared in different rotational states typically experience different trapping potentials and therefore are subject to undesirable decoherence, leading to short coherence times [28–30]; (2) fine tuning of the many-body Hamiltonian parameters requires the use of strong and well-controlled dc electric fields E [1, 11]. As these fields take time to switch and change, on-demand generation of entanglement using long-range ED interactions between rotational states remains a significant experimental challenge.

To overcome these important limitations, here we propose to leverage a larger set of internal levels accessible in ultracold polar molecules, which include nuclear and/or electron spin levels in addition to their rotational structure. Taken together, these levels can be used as a robust resource for on-demand entanglement generation. By encoding an effective spin-1/2 into a combined set of nuclear spin and rotational molecular levels, we take advantage of the long coherence times enjoyed by nuclear spin levels and the strong ED interactions experienced by rotational levels at different stages of the entanglement generation process. We note that other types of qubit encodings have been suggested in Refs. [4, 5]. Our

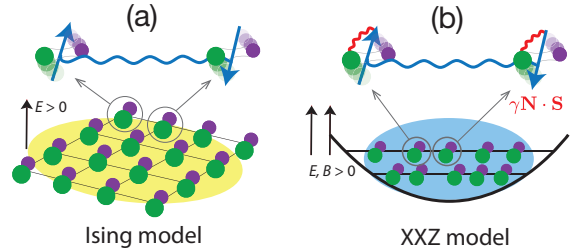


FIG. 1. (a) Experimental setup for nuclear spin entanglement generation consisting of $^1\Sigma$ molecules in superpositions of spin-rotational states trapped in an optical lattice on a 2D plane. Molecular spins (arrows) interact via the long-range Ising interaction (wavy line), creating cluster-state entanglement represented by the yellow shaded area. (b) Same as (a) but in the presence of a B -field and the spin-rotation interaction (red wavy lines) near an avoided crossing. The blue shaded area represents entanglement of the XXZ type leading to the generation of spin-squeezed states.

proposal, in addition to the electric tunability of dipole-induced spin-exchange and Ising couplings, offers magnetic tunability of the ED interactions, and the ability to turn off exchange interactions on demand even at finite E -fields. The magnetic tunability, an essential advantage of our approach, arises from inducing avoided crossings of electron spin-rotational levels of the opposite parity in $^2\Sigma$ molecules such as YO [31–34], CaF [35, 36], and SrF [37, 38], which have already been cooled down and trapped in optical potentials. We also show how to engineer magnetically tunable level crossings in $^1\Sigma$ molecules via mw dressing. In this way, we can engineer spin models of Ising and XXZ types with an enlarged set of control parameters.

Entangling nuclear spins of $^1\Sigma$ molecules: Ising interactions and cluster states. Consider an ensemble of ultracold $^1\Sigma$ molecules confined to a single plane of a three-dimensional (3D) optical lattice at unit filling as shown in Fig. 1(a). To entangle the nuclear spins of the molecules via ED interactions, we propose to encode an effective spin-1/2 into the states $|\uparrow\rangle = |\tilde{0}0, M\rangle$ and $|\downarrow\rangle = |\tilde{1}0, M'\rangle$ as shown in Fig. 2(a). We refer to these

states as nuclear spin-rotational states. Here, $|\tilde{N}M_N, M\rangle$ denote molecular eigenstates in the limit of large magnetic field B , where the nuclear spin projections on the field axis $M = \{M_{I_1}, M_{I_2}\}$ are good quantum numbers [26, 39]. At zero E -field the rotational quantum number N is a good quantum number with the rotational energy spacing set by the rotational constant B_e . At finite E -field, the rotational states admix but we can still label the states that adiabatically connect to zero-field N -states as \tilde{N} [40]. We further assume that the external E and B -fields are parallel, so that M_N , the projection of \mathbf{N} on the field axis, is always a good quantum number.

Importantly, we require that our effective spin-1/2 states have *different* nuclear spin projections ($M \neq M'$), which ensures that the off-diagonal matrix elements of the molecular electric dipole moment (EDM) \hat{d} are strongly suppressed ($d_{\uparrow\downarrow} \rightarrow 0$). This is because in the large B -field limit, the electric quadrupole interaction, which couples states with different M and M_N , is small compared to the Zeeman interaction [41]. This property makes our encoding distinct from the one proposed in all of the previous theoretical work, which used rotational states with $M = M'$ [1–4, 6–8, 11]. The only exception is Ref. [42], which proposed the use of a combination of electron spin and rotational states near avoided level crossings to engineer interqubit interactions using infrared laser pulses. In our work, these interactions arise naturally without the need to use extra pulses or avoided crossings (except in the specific case of the XXZ model with $^1\Sigma$ molecules as discussed below).

In the absence of an external E -field, all matrix elements of the EDM vanish identically since our nuclear spin-rotational qubit states [see Fig. 2(a)] have a definite parity. As a result, the long-range ED interaction between the molecules also vanishes. When an E -field is applied, the diagonal matrix elements $d_{\uparrow} = \langle \uparrow | \hat{d} | \uparrow \rangle$ and $d_{\downarrow} = \langle \downarrow | \hat{d} | \downarrow \rangle$ acquire finite values with $d_{\uparrow} \neq d_{\downarrow}$, as shown in Fig. 2(b), whereas $d_{\uparrow\downarrow} \rightarrow 0$ (see above). As shown in the Supplemental Material [41], this leads to the emergence of the ED interactions between molecules in the different nuclear spin-rotational states described by the long-range Ising model

$$\hat{H}_{\text{dip}} = \sum_{i>j} J_{ij}^z \hat{S}_i^z \hat{S}_j^z \quad (1)$$

where the effective spin-1/2 operators \hat{S}_i^z act in the two-dimensional Hilbert space of the i -th molecule $\{|\downarrow\rangle, |\uparrow\rangle\}$, $J_{ij}^z = \frac{1-3\cos^2\theta_{ij}}{|\mathbf{R}_{ij}|^3} (d_{\uparrow} - d_{\downarrow})^2$ is the Ising coupling constant, \mathbf{R}_{ij} is the distance vector between the molecular centers of mass, and θ_{ij} is the angle between \mathbf{R}_{ij} and the direction of the E -field. The E -field dependence of J_{ij}^z shown in Fig. 2(b) reaches a maximum at $\beta_E = Ed/B_e \simeq 3$.

Importantly, because our effective spin-1/2 states correspond to the $\tilde{N} = 0$ and $\tilde{N} = 1$ Stark levels, the Ising interaction between the molecules in different nu-

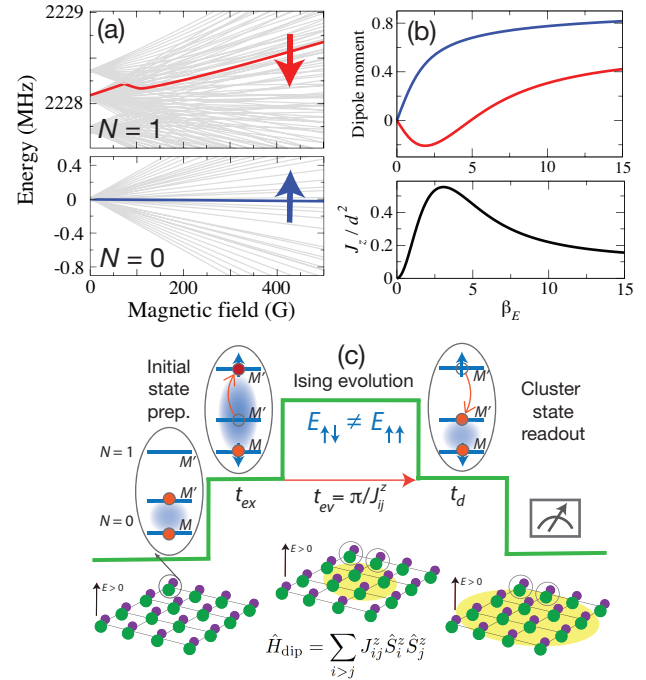


FIG. 2. (a) Zeeman energy levels of a typical bialkali molecule (here, $^{40}\text{K}^{87}\text{Rb}$). Our effective spin-1/2 states $|\uparrow\rangle = |\tilde{0}0, M\rangle$ and $|\downarrow\rangle = |\tilde{1}0, M'\rangle$ are marked by arrows. (b) Expectation values of the EDM d_{\uparrow} (top curve) and d_{\downarrow} (lower panel) and the Ising coupling constant J_z (bottom panel) as a function of the reduced E -field strength $\beta_E = dE/B_e$ [40]. (c) Protocol for creating long-lived nuclear spin cluster states of polar molecules via ED interactions.

clear spin-rotational states ($M \neq M'$) is as strong as that between the molecules in ordinary rotational states ($M = M'$) [10].

The starting point of our general entanglement-generating protocol is an ensemble of $\tilde{N} = 0$ molecules trapped in a single plane of a 3D optical lattice as shown in Fig. 2(c). The molecules are initialized in a coherent superposition of two different $\tilde{N} = 0$ nuclear spin states $|\tilde{0}0, +\rangle = \frac{1}{\sqrt{2}}[|\tilde{0}0, M\rangle + |\tilde{0}0, M'\rangle]$. No long-range interactions are initially present between the molecules, since $d_{\uparrow} = d_{\downarrow}$ for all $\tilde{N} = 0$ nuclear spin states even in the presence of a dc E -field, and thus $J_{ij}^z = 0$. As an example, we consider ultracold KRb($^1\Sigma^+$) molecules prepared in a coherent superposition of two nuclear spin states $|\tilde{0}0, +\rangle_{\text{KRb}} = \frac{1}{\sqrt{2}}[|\tilde{0}0, -3, -\frac{1}{2}\rangle + |\tilde{0}0, -4, \frac{1}{2}\rangle]$, which can be realized experimentally via two-photon microwave excitation [26, 43].

In *Step 1*, we initialize our spin-rotational qubits by preparing a coherent superposition $|\+\rangle = \frac{1}{\sqrt{2}}[|\uparrow\rangle + |\downarrow\rangle]$ [see Fig. 2(c)]. This can be achieved by starting with the coherent superposition of $\tilde{N} = 0$ nuclear spin states $|\tilde{0}0, +\rangle$ defined above, and applying a resonant pulse of mw radiation on the $|\tilde{0}0, M'\rangle \rightarrow |\tilde{1}0, M'\rangle$ rotational transition.

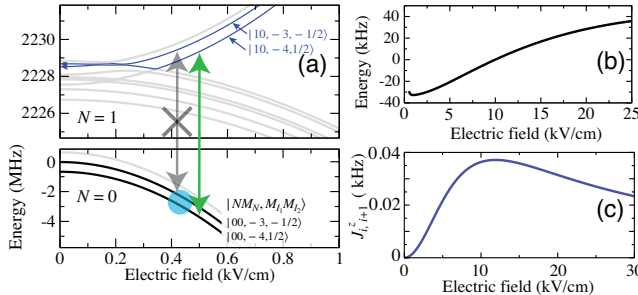


FIG. 3. (a) Energy levels of $^{40}\text{K}^{87}\text{Rb}$ used in our entanglement generation protocol plotted vs E -field at $B = 400$ G and $M_F = M_N + M_{I_{\text{K}}} + M_{I_{\text{Rb}}} = -7/2$. The initial coherent superposition of the $\tilde{N} = 0$ nuclear spin states is marked with a blue circle. The mw transition used to excite the initial coherent superposition $|+\rangle$ is marked with a green arrow. The competing mw transition is marked by the grey arrow. The differential Stark shift (b) and the NN Ising constant (c) plotted vs E -field for $^{40}\text{K}^{87}\text{Rb}$ molecules at the lattice spacing of 500 nm.

Figure 3(a) illustrates the idea for KRb. By applying a mw π pulse to the superposition $|\tilde{0}0, +\rangle_{\text{KRb}}$ resonant on the $|\tilde{0}0, -4, \frac{1}{2}\rangle \rightarrow |\tilde{1}0, -4, \frac{1}{2}\rangle$ transition (which has a large transition dipole moment), the population in the $|\tilde{0}0, -4, \frac{1}{2}\rangle$ state is coherently transferred to the rotationally excited state, leading to the desired superposition $|+\rangle_{\text{KRb}} = \frac{1}{\sqrt{2}}[|\tilde{0}0, -3, -\frac{1}{2}\rangle + |\tilde{1}0, -4, \frac{1}{2}\rangle]$. To show that it is possible to selectively excite a single eigenstate component of the initial superposition, (i.e. $|\tilde{0}0, -4, \frac{1}{2}\rangle$ but not $|\tilde{0}0, -3, -\frac{1}{2}\rangle$), we plot in Fig. 3(b) the energy difference between the main transition ($|\tilde{0}0, -4, \frac{1}{2}\rangle \leftrightarrow |\tilde{1}0, -4, \frac{1}{2}\rangle$) and the competing transition. The differential Stark shift is seen to be negative at small E -fields, approaching zero at $E \simeq 10$ kV/cm. Thus, selective mw excitation of the desired transition $|\tilde{0}0, -4, \frac{1}{2}\rangle \rightarrow |\tilde{1}0, -4, \frac{1}{2}\rangle$ is possible by tuning the E -field below 5 kV/cm or above 15 kV/cm, where the competing transition is energetically detuned.

In Step 2, we let our initial n -molecule superposition $|+\rangle^{\otimes n}$ evolve under the Ising interaction for the cluster time $t_c = \pi/|J_{i,i+1}^z|$. Because of the long-range nature of the interaction, the resulting proxy cluster state will be different from the proper cluster state formed under nearest-neighbor (NN) interactions [20, 21]. Nevertheless, theoretical simulations show that cluster-state fidelities above 75% can be achieved for ≤ 12 molecules even in the presence of moderately strong ($|J_{i,i+2}^z/J_{i,i+1}^z| = 0.1$) next-NN interactions [44]. These interactions can also be efficiently suppressed using dynamical decoupling techniques [44].

At $t = t_c$ a maximally entangled cluster state of nuclear spin-rotational qubits is created [20, 24]. The Ising coupling constant $J_{i,i+1}^z$ is plotted for the NN interactions of KRb molecules in Fig. 3(c). At $E = 20$ kV/cm and the NN spacing of 500 nm, $J_{i,i+1}^z/2\pi = 30$ Hz and it takes $t_c \simeq 16.7$ ms to evolve the lattice-confined ensem-

ble of KRb molecules into the highly entangled cluster state. Preserving the coherence during Ising evolution is experimentally feasible because the coherence times T_2 of the nuclear spin-rotational superpositions are likely to be similar to those of purely rotational superpositions [43, 45], with $T_2 \simeq 1$ s theoretically achievable [29] using state-insensitive (“magic”) trapping conditions [28].

In Step 3, we coherently transfer population back to the ground rotational state via the $|\tilde{1}0, M'\rangle \rightarrow |\tilde{0}0, M'\rangle$ transition. After the deexcitation step, the molecules find themselves once again in a coherent superposition of $\tilde{N} = 0$ nuclear spin sublevels $|\tilde{0}0, +\rangle = \frac{1}{\sqrt{2}}[|\tilde{0}0, M\rangle + |\tilde{0}0, M'\rangle]$. The long-range Ising interaction is thereby completely turned off, preserving the entanglement created in Step 2. We expect the resultant nuclear spin cluster state to be both long-lived and robust due to the much longer coherence times of $\tilde{N} = 0$ nuclear spin qubits compared to their rotational counterparts [43, 45]. These advantages of our protocol enable long-term storage of quantum information in the cluster state encoded in molecular nuclear spins, enabling efficient implementation of the measurement protocols of one-way quantum computing [21, 22].

We next consider the question of how to engineer a more general XXZ-type interaction between the electron spins of $^2\Sigma$ molecules or nuclear spins of $^1\Sigma$ molecules. While the XXZ interaction arises naturally between the different rotational states with $M = M'$ [11, 40] it requires finite off-diagonal EDM matrix elements, which are absent in the basis of nuclear spin-rotation states we have considered so far. Thus, in order to obtain a nonzero spin exchange coupling, it is necessary to break the spin symmetry. Here, we consider two symmetry-breaking scenarios that rely on the spin-rotation interaction in $^2\Sigma$ molecules and on mw-dressed rotational states of $^1\Sigma$ molecules.

As a specific example, consider the $\text{YO}(^2\Sigma)$ molecule recently laser cooled [33] and trapped in an optical lattice [34]. A remarkable feature of YO is its extremely large hyperfine interaction, which dominates over the spin-rotation interaction and results in the total spin angular momentum $\mathbf{G} = \mathbf{I} + \mathbf{S}$ being a good quantum number [32] at low B -fields, where \mathbf{I} and \mathbf{S} are the nuclear and electron spins, respectively. In the large B -field limit, the spin-rotational states of $\text{YO}(^2\Sigma)$ $|\tilde{N}M_N M_S M_I\rangle$, have well-defined values of nuclear (M_I) and electron (M_S) spin projections on the field axis.

Figure 4(a) shows the lowest rotational energy levels of $\text{YO}(^2\Sigma)$. The opposite-parity levels $|\tilde{0}0\frac{1}{2}M_I\rangle$ and $|\tilde{1}1-\frac{1}{2}M_I\rangle$ cross at $B_c \simeq 0.85$ T [46–48]. At $B = B_c$ and $E > 0$, the electron spin-rotation interaction mixes the levels, leading to an avoided level crossing (ALC) shown in Fig. 4(b), and we choose our effective spin-1/2 states $|\alpha\rangle = |\uparrow\rangle, |\downarrow\rangle$ as

$$|\alpha\rangle = c_{\alpha 1} |\tilde{0}0\frac{1}{2}M_I\rangle + c_{\alpha 2} |\tilde{1}1-\frac{1}{2}M_I\rangle, \quad (2)$$

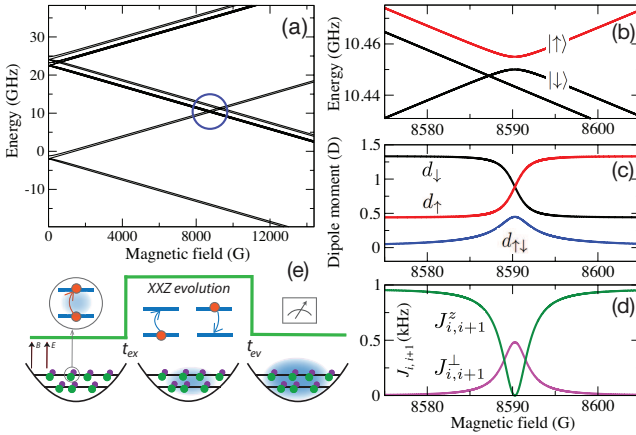


FIG. 4. (a) Zeeman energy levels of YO at $E = 5$ kV/cm. The ALC between the levels $|\tilde{0}0\frac{1}{2}M_I\rangle$ and $|\tilde{1}1-\frac{1}{2}M_I\rangle$ is marked with a circle. Energy levels (b), EDM matrix elements (c), and NN spin coupling constants $J_{i,i+1}^z$ and $J_{i,i+1}^\perp$ (d) plotted as a function of B -field near the ALC at the NN spacing of 500 nm. (e) Experimental protocol for creating long-lived spin-squeezed states of YO molecules.

where $c_{\alpha i}$ are B -dependent mixing amplitudes [41]. Thus, in the vicinity of the ALC, the electron spin and rotation mixing provides $d_{\uparrow\downarrow} \neq 0$, which gives rise to the XXZ interaction [41]

$$\hat{H}_{\text{dip}}^{\text{ex}} = \sum_{i>j} \left[\frac{1}{2} J_{ij}^\perp (\hat{S}_i^+ \hat{S}_j^- + \text{H.c.}) + J_{ij}^z \hat{S}_i^z \hat{S}_j^z \right], \quad (3)$$

where $J_{ij}^\perp = \frac{1-3\cos^2\theta_{ij}}{|\mathbf{R}_{ij}|^3} 2d_{\uparrow\downarrow}^2$ is the spin-exchange coupling constant. As shown in Figs. 4(c)-(d), because the spin mixing in Eq. (2) is localized in the vicinity of the ALC, both $d_{\uparrow\downarrow}$ and J_{ij}^\perp peak at $B = B_c$, where $|c_{\alpha i}| = 1/\sqrt{2}$. The diagonal matrix elements of the EDM become equal at $B = B_c$, where J_{ij}^z vanishes [see Fig. 4(d)]. The remarkable magnetic tunability of the spin coupling constants near ALCs can be used to vary the ratio J_{ij}^z/J_{ij}^\perp over a wide range. Achieving such tuning of J_{ij}^z/J_{ij}^\perp is highly desirable for, e.g., accessing new regimes of spin-squeezing dynamics [49] and quantum simulation, since its tunability is far from straightforward in traditional protocols that rely on pure rotational states, requiring the use of multiple mw fields [11].

To realize the spin-squeezed states experimentally, we propose to use a standard Ramsey protocol shown in Fig. 4(e), in which mw fields are used to excite the initial coherent superposition $\frac{1}{\sqrt{2}}[|\uparrow\rangle + |\downarrow\rangle]$ (as recently realized in a beam experiment [50]) and during the dark time the system is let to evolve under the XXZ Hamiltonian.

The evolution leads to the formation of a spin-squeezed state in the $\{|\uparrow\rangle, |\downarrow\rangle\}$ basis [19]. At the last step, the B -field is adiabatically ramped down to transfer the $|\uparrow\rangle$ and $|\downarrow\rangle$ states back to the $|\tilde{0}0\frac{1}{2}M_I\rangle$ and $|\tilde{1}1-\frac{1}{2}M_I\rangle$ zeroth-order states, and the latter state is coherently transferred

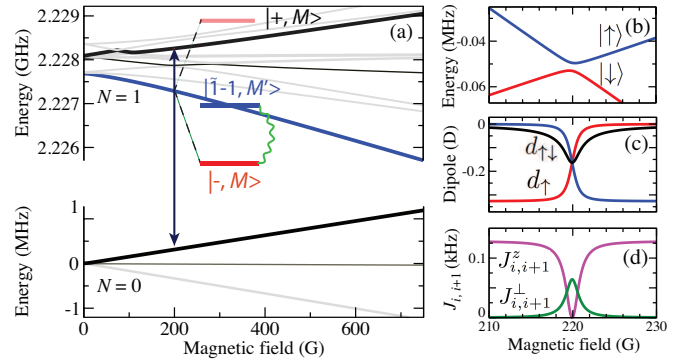


FIG. 5. (a) Mw-dressed states $|\pm, M\rangle$ (red bars) of ${}^{40}\text{K}{}^{87}\text{Rb}$ for $M_F = 7/2$ obtained by driving the mw transition (vertical arrow, $\Omega/2\pi = 2.1$ MHz) between the bare levels $|\tilde{0}0, -2, -\frac{3}{2}\rangle$ and $|\tilde{1}0, -2, -\frac{3}{2}\rangle$. The effective spin-1/2 is encoded into the mw-dressed state $|-, M\rangle$ and the bare state $|\tilde{1}1-1, -4, \frac{3}{2}\rangle$ (blue bar), which are coupled by the electric quadrupole interaction (wavy line). B -field dependence of the effective spin-1/2 energy levels (b), EDM matrix elements (c), and NN XXZ spin coupling constants $J_{i,i+1}^\perp$ and $J_{i,i+1}^z$ (d) near the ALC.

to the $|\tilde{0}0 - \frac{1}{2}M_I\rangle$ state using a circularly polarized mw π -pulse. As a result, we obtain a long-lived squeezed state of electron spins of $\tilde{N} = 0$ ${}^2\Sigma$ molecules, which can be used to measure, e.g., external B -fields.

The above scenario of generating magnetically tunable XXZ interactions is clearly unfeasible for ${}^1\Sigma$ molecules due to their extremely small nuclear magnetic moments. To overcome this limitation, we use mw dressing to make the opposite-parity states degenerate as illustrated in Fig. 5(a). Specifically, driving the transition between the states $|\tilde{0}0, M\rangle$ and $|\tilde{1}0, M\rangle$ (such as the $|\tilde{0}0, -2, -\frac{3}{2}\rangle$ and $|\tilde{1}0, -2, -\frac{3}{2}\rangle$ states of KRb) by a linearly polarized mw field creates a pair of mw-dressed states in the rotating frame [10]

$$|\pm, M\rangle = c_0^\pm(\Omega, \Delta) |\tilde{0}0, M\rangle + c_1^\pm(\Omega, \Delta) |\tilde{1}0, M\rangle, \quad (4)$$

where the mixing coefficients $c_{\tilde{N}}^\pm$ depend on the Rabi frequency Ω and the detuning from resonance Δ . For simplicity, we will consider the case of resonant driving ($\Delta = 0$), where the energies of the mw-dressed states $E_\pm = E_{1,M} \pm \Omega/2$ (assuming $\hbar = 1$), and $E_{1,M}$ is the energy of the bare state $|\tilde{1}0, M\rangle$. We note that the coherence time of these states could be limited by the different trapping potentials experienced by the $|\tilde{0}0, M\rangle$ and $|\tilde{1}0, M\rangle$ bare states, as well as by the coherence properties of the dressing field. Fortunately, it may be possible to choose the mixing coefficients $c_{\tilde{N}}^\pm$ in such a way as to achieve state-insensitive trapping conditions [11, 51].

To encode the effective spin-1/2, we choose the lowest-energy mw-dressed state $|-, M\rangle$ defined above and the bare state $|\tilde{1}1-1, M'\rangle = |\tilde{1}1-1, -4, \frac{3}{2}\rangle$ of KRb shown in Fig. 5(a). These states are coupled by the electric quadrupole interaction [41] via the matrix element

$V_{MM'} = \langle -, M | \hat{H}_{eQ} | \tilde{1} - 1, M' \rangle = 1.8$ kHz. Figure 5(b) shows the energies of our effective spin-1/2 states $|\uparrow, \downarrow\rangle = c_M^{(\uparrow\downarrow)} |-, M\rangle + c_{M'}^{(\uparrow\downarrow)} |\tilde{1} - 1, M'\rangle$ as a function of B -field. The NN spin coupling constants $J_{i,i+1}^\perp$ and $J_{i,i+1}^z$ shown in Fig. 5(d) reach their maximal and minimal values at $B = B_c$. We note that $J_{ij}^z(B_c) = 0$ since $d_\uparrow = d_\downarrow$ at the ALC, and thus the ratio $J_{i,i+1}^\perp/J_{i,i+1}^z$ can be magnetically tuned over a wide dynamic range.

In summary, we have shown how to engineer long-lived

cluster and spin-squeezed states using the nuclear spins of ${}^1\Sigma$ molecules and the electron spins of ${}^2\Sigma$ molecules in their ground rotational states. The proposed schemes can be applied to a wide range of polar molecules recently cooled and trapped in many laboratories, opening up a general path to long-lived spin entanglement generation in ultracold molecular ensembles.

Acknowledgements. This work was supported by the NSF EPSCoR RII Track-4 Fellowship (Award No. 1929190) and by NIST.

Supplemental Material

In this Supplemental Material, we present technical details concerning molecular Hamiltonians and the computation of the energy levels of KRb and YO molecules in the presence of external electric and magnetic fields (Sec. I). We also provide a derivation of the interaction Hamiltonian between polar ${}^2\Sigma$ molecules near avoided level crossings (ALCs) of their opposite-parity Zeeman states. To this end, Sec. IIA begins with a derivation of the effective single-molecule Hamiltonian near an ALC. In Sec. IIB, we derive the electric dipole-dipole interaction between the molecules, and show that it takes the form of the XXZ spin model in the immediate vicinity of an ALC, and of the quantum Ising model far away from the ALC.

HAMILTONIANS AND ENERGY LEVELS OF ${}^1\Sigma$ AND ${}^2\Sigma$ MOLECULES IN ELECTRIC AND MAGNETIC FIELDS

${}^1\Sigma$ molecules (KRb)

To calculate the energy levels of KRb(${}^1\Sigma^+$) as a function of external dc electric and magnetic fields, we use the effective Hamiltonian for the ground vibrational state [39]

$$\hat{H}_{\text{mol}} = B_e \hat{N}^2 + \hat{H}_{\text{hf}} + \hat{H}_E + \hat{H}_B, \quad (1)$$

where the first term describes the rotational energy of the molecule, B_e is the rotational constant, and \hat{N} is the rotational angular momentum operator. The second term in Eq. (1) represents the hyperfine interaction, and the third and fourth terms describe the interaction of the molecule with external dc electric and magnetic fields.

The hyperfine Hamiltonian is given by

$$\hat{H}_{\text{hf}} = \hat{H}_{eQ} + \hat{H}_{IN} + \hat{H}_{ss,t} + \hat{H}_{ss,d}, \quad (2)$$

where the first term on the right-hand side stands for the electric quadrupole interaction, the second term for the nuclear spin-rotation interaction, the third term for the scalar spin-spin interaction, and the fourth term for the tensor spin-spin interaction. The electric quadrupole interaction provides the dominant contribution to the hyperfine coupling in KRb ($\simeq 1$ MHz), followed by the nuclear spin-rotation and scalar spin-spin couplings (10s of kHz) and by the tensor spin-spin coupling ($\simeq 10$ Hz).

The Zeeman interaction of the molecule with an external magnetic field is given by

$$\hat{H}_B = -g_r \mu_N B N_z - g_1 \mu_N B I_{1z} (1 - \sigma_1) - g_2 \mu_N B I_{2z} (1 - \sigma_2) \quad (3)$$

where $I_{\nu z}$ are the nuclear spin angular momentum operators along the z -axis defined by the external magnetic field vector \mathbf{B} , the subscripts $\nu = 1, 2$ refer to the individual nuclei (K and Rb), $B = |\mathbf{B}|$, g_r is the rotational g -factor, g_i are the nuclear g -factors, σ_i are the diagonal elements of the nuclear shielding tensor [39], and μ_N is the nuclear Bohr magneton.

Finally, the interaction of the molecule with an external electric field is described by

$$\hat{H}_E = -\mathbf{E} \cdot \mathbf{d} = -Ed \cos \theta, \quad (4)$$

where d is the magnitude of the electric dipole moment vector \mathbf{d} , \mathbf{E} is the electric field vector, and θ is the angle between the molecular axis and the quantization axis defined by \mathbf{E} . We assume that the electric and magnetic field vectors are parallel ($\mathbf{E} \parallel \mathbf{B}$).

The molecular constants that parametrize the Hamiltonian (1) are taken from Ref. [39] for the fermionic $^{40}\text{K}^{87}\text{Rb}$ isotope. To compute the energy levels we constructed and diagonalized the Hamiltonian in the uncoupled basis $|NM_N\rangle|I_1M_{I_1}\rangle|I_2M_{I_2}\rangle$ using the expressions for the matrix elements from Ref. [11]. A total of 5 rotational basis states are included in the basis to produce converged energy levels at electric fields up to 30 kV/cm. To verify our computed energy levels, we compared them to the data shown in Fig. 1 of Ref. [52] and found good agreement.

$^2\Sigma$ molecules (YO)

The Hamiltonian of a $^2\Sigma$ molecule such as YO($^2\Sigma^+$) is given by [31]

$$\hat{H}_{\text{mol}} = B_e \hat{N}^2 + \gamma \hat{\mathbf{N}} \cdot \hat{\mathbf{S}} + \hat{H}_{\text{hf}} + \hat{H}_E + \hat{H}_B, \quad (5)$$

where the first term represents the rotational energy, and the second term describes the spin-rotation interaction of \mathbf{N} with \mathbf{S} , the electron spin angular momentum of the molecule, whose strength is quantified by the spin-rotation constant γ . The hyperfine interaction is given by the third term in Eq. (5), whereas the interaction of the molecule with external dc electric and magnetic fields is described by the third and fourth terms. The hyperfine interaction has the form

$$\hat{H}_{\text{hf}} = (b + c/3) \mathbf{I} \cdot \mathbf{S} + c \frac{\sqrt{6}}{3} \left(\frac{4\pi}{5} \right)^{1/2} \sum_q (-1)^q Y_{2,-q}(\mathbf{r}) [\mathbf{I} \otimes \mathbf{S}]_q^{(2)}, \quad (6)$$

where b and c are the isotropic and anisotropic hyperfine constants, respectively, \mathbf{r} describes the orientation of the molecular axis in the laboratory frame with the z -axis defined by the external magnetic fields (see above), $Y_{2,-q}$ is a spherical harmonic, and $[\mathbf{I} \otimes \mathbf{S}]_q^{(2)}$ is a second-rank tensor product of the electron and nuclear spin operators [53]. The hyperfine interaction in YO is remarkably strong, making the total spin $|\mathbf{G}| = |\mathbf{I} + \mathbf{S}|$ a good quantum number in the weak B -field limit. The interaction with an external magnetic field $\hat{H}_B = g_S \mu_0 B \hat{S}_z$, where μ_0 is the Bohr magneton and $g_S \simeq 2$ is the electron spin g -factor.

The molecular constants B_e , γ , b , and c for YO are taken from Ref. [31] and the Hamiltonian (1) is represented in the basis $|NM_N\rangle|SM_S\rangle|IM_I\rangle$ composed of eigenstates of \mathbf{N}^2 and \hat{N}_z , \mathbf{S}^2 and \hat{S}_z , and \mathbf{I}^2 and \hat{I}_z .

The matrix elements of the operators in Eq. (5) are evaluated as described in Ref. [54]. Numerical diagonalization of the Hamiltonian matrix provides the energy levels of YO in good agreement with the literature data from Ref. [31].

DERIVATION OF SINGLE-MOLECULE EFFECTIVE HAMILTONIAN AND OF THE SPIN LATTICE HAMILTONIAN FOR $^2\Sigma$ MOLECULES NEAR AVOIDED CROSSINGS

Effective Hamiltonian for a single $^2\Sigma$ molecule in its ground rovibrational state near an ALC

Consider a single $^2\Sigma$ molecule in superimposed electric and magnetic fields described by the Hamiltonian [46–48]

$$\hat{H}_{\text{mol}} = B_e \hat{N}^2 + \gamma \hat{\mathbf{N}} \cdot \hat{\mathbf{S}} - g_S \mu_0 B \hat{S}_z - \hat{\mathbf{d}} \cdot \mathbf{E} \quad (7)$$

where $\hat{\mathbf{N}}$ and $\hat{\mathbf{S}}$ are the rotational and spin angular momentum operators of the molecule, B_e is the rotational constant, γ is the spin-rotation constant, $g_S \simeq 2.0$ is the g -factor, and μ_0 is the Bohr magneton. The quantization axis in Eq. (7) is chosen along the direction of the external magnetic field, which is assumed to be parallel to the electric field. We will neglect the molecular hyperfine structure, which is an excellent approximation at large magnetic fields required to induce avoided crossings between the different rotational levels in $^2\Sigma$ molecules. For example, in YO($^2\Sigma^+$), which has an extremely large hyperfine interaction, the level crossings occur near 8500 G [see Figs. 4(a) and 4(b) of the main text], where the nuclear spin is completely decoupled from the electron spin and from molecular rotation, and thus M_I remains a good quantum number. Because the molecular Hamiltonian does not couple the states $|\tilde{0}0\frac{1}{2}M_I\rangle$ and $|\tilde{1}1-\frac{1}{2}M'_I\rangle$ involved in the ALC unless $M_I = M'_I$, the ALCs can only occur between the states of the same M_I .

We will use the basis $|NM_N\rangle|SM_S\rangle = |NM_NM_S\rangle$, where $|NM_N\rangle$ are the eigenstates of \hat{N}^2 and \hat{N}_z and $|SM_S\rangle$ are those of \hat{S}^2 and \hat{S}_z [we will omit the label S since $S = 1/2$ for $^2\Sigma^+$ molecules]. Near the ALC between the opposite-parity Zeeman levels [see Fig. 4(b) of the main text], we only need to take into account three basis states in

the weak E -field limit: $|00\frac{1}{2}\rangle$, $|10\frac{1}{2}\rangle$, and $|11 - \frac{1}{2}\rangle$. In this basis, the matrix of the molecular Hamiltonian (7) takes the form [48]

$$H_{\text{mol}} = \begin{pmatrix} \mu_0 B & -Ed/\sqrt{3} & 0 \\ -Ed/\sqrt{3} & 2B_e + \mu_0 B & \gamma/\sqrt{2} \\ 0 & \gamma/\sqrt{2} & 2B_e - \mu_0 B - \gamma/2 \end{pmatrix}. \quad (8)$$

Here, the basis states $|00\frac{1}{2}\rangle$ and $|10\frac{1}{2}\rangle$ are coupled by an external electric field and the basis states $|10\frac{1}{2}\rangle$, and $|11 - \frac{1}{2}\rangle$ are coupled by the spin-rotation interaction.

In the weak electric field limit, where $\beta_E = Ed/B_e \ll 1$, we can define the zeroth-order Zeeman states, which do not interact except in close vicinity of the ALC:

$$\begin{aligned} |\tilde{0}0\frac{1}{2}\rangle &= c_0 |00\frac{1}{2}\rangle + c_1 |10\frac{1}{2}\rangle, \\ |\tilde{1}1 - \frac{1}{2}\rangle &= |11 - \frac{1}{2}\rangle. \end{aligned} \quad (9)$$

where we have neglected the electric field coupling between the $N = 1$ and $N = 2$ rotational states, since it does not affect the interaction between the states (9) to first order in β_E .

Projecting the molecular Hamiltonian (7) onto the zeroth-order basis (9) and using Eq. (8) we obtain the matrix elements

$$\begin{aligned} \langle \tilde{0}0\frac{1}{2} | \hat{H}_{\text{mol}} | \tilde{0}0\frac{1}{2} \rangle &= c_0^2 \mu_0 B + 2c_0 c_1 (-Ed/\sqrt{3}) + c_1^2 (2B_e + \mu_0 B), \\ \langle \tilde{0}0\frac{1}{2} | \hat{H}_{\text{mol}} | \tilde{1}1 - \frac{1}{2} \rangle &= c_1 \langle 10\frac{1}{2} | \hat{H}_{\text{mol}} | 11 - \frac{1}{2} \rangle = c_1 \gamma/\sqrt{2}, \\ \langle \tilde{1}1 - \frac{1}{2} | \hat{H}_{\text{mol}} | \tilde{1}1 - \frac{1}{2} \rangle &= \langle 11 - \frac{1}{2} | \hat{H}_{\text{mol}} | 11 - \frac{1}{2} \rangle = 2B_e - \mu_0 B - \gamma/2. \end{aligned} \quad (10)$$

These equations can be simplified in the weak E -field limit, where $c_0 \rightarrow 1$ and $c_1 \rightarrow Ed/(2\sqrt{3}B_e)$ [40]:

$$\begin{aligned} \langle \tilde{0}0\frac{1}{2} | \hat{H}_{\text{mol}} | \tilde{0}0\frac{1}{2} \rangle &= \mu_0 B - \frac{(Ed)^2}{6B_e}, \\ \langle \tilde{0}0\frac{1}{2} | \hat{H}_{\text{mol}} | \tilde{1}1 - \frac{1}{2} \rangle &= \frac{Ed\gamma}{2\sqrt{6}B_e}, \\ \langle \tilde{1}1 - \frac{1}{2} | \hat{H}_{\text{mol}} | \tilde{1}1 - \frac{1}{2} \rangle &= 2B_e - \mu_0 B - \gamma/2. \end{aligned} \quad (11)$$

Thus, the energy level structure of a ${}^2\Sigma$ molecule near the lowest-energy ALC of its opposite-parity Zeeman levels is described by the following effective Hamiltonian in the zeroth-order basis $\{|\tilde{0}0\frac{1}{2}\rangle, |\tilde{1}1 - \frac{1}{2}\rangle\}$

$$H_{\text{eff}} = \begin{pmatrix} \mu_0 B - (Ed)^2/(6B_e) & Ed\gamma/(2\sqrt{6}B_e) \\ Ed\gamma/(2\sqrt{6}B_e) & 2B_e - \mu_0 B - \gamma/2 \end{pmatrix} \quad (12)$$

The diagonal matrix elements of the effective Hamiltonian give the energies of zeroth-order Zeeman levels, which become equal at the crossing point defined by $2\mu_0 B_c = 2B_e - \gamma/2 + (Ed)^2/(6B_e)$. The off-diagonal matrix element $Ed\gamma/(2\sqrt{6}B_e)$ quantifies the coupling between the zeroth-order Zeeman levels, which requires both the electric field (to couple the spatial components of bare $N = 0$ and $N = 1$ rotational states) and the spin-rotation interaction (to couple the spin components of the $N = 1$ rotational states).

The eigenstates near the ALC, $|\alpha\rangle = \{|\uparrow\rangle, |\downarrow\rangle\}$, can be obtained by diagonalizing the effective Hamiltonian (12)

$$|\alpha\rangle = c_{\alpha\tilde{0}} |\tilde{0}0\frac{1}{2}\rangle + c_{\alpha\tilde{1}} |\tilde{1}1 - \frac{1}{2}\rangle, \quad (13)$$

where $(c_{\alpha\tilde{0}}, c_{\alpha\tilde{1}})^T$ are the eigenvectors of the 2×2 effective Hamiltonian matrix (12) corresponding to the eigenvalues E_α . At the crossing point ($B = B_c$) the diagonal matrix elements are degenerate, and thus even an arbitrarily small electric field results in a complete mixing of the opposite-parity states ($|c_{\alpha i}| = 1/\sqrt{2}$). The effective spin-1/2 states near the ALC are thus linear combinations of the zeroth-order Zeeman states of the opposite parity and spin.

Effective spin-spin interactions and spin lattice Hamiltonian for $^2\Sigma$ molecules near avoided level crossings

In this section, we derive the electric dipolar (ED) interaction Hamiltonian and the many-body spin Hamiltonian for polar $^2\Sigma$ molecules in the vicinity of an ALC. We begin by considering two $^2\Sigma$ molecules i and j with the dipole moment operators \hat{d}_i and \hat{d}_j interacting via the ED interaction. Assuming that the interaction is much smaller than the energy gap between our effective spin-1/2 states at the ALC (true in our case), we can restrict attention to energy-conserving resonant exchange terms, and consider only the $q = 0$ tensor component of the ED interaction [40]:

$$\hat{H}_{\text{dip},ij}^{(q=0)} = \frac{1-3\cos^2\theta_{ij}}{R_{ij}^3} \left[\frac{1}{2} (\hat{d}_i^{(1)} \hat{d}_j^{(-1)} + \hat{d}_i^{(-1)} \hat{d}_j^{(1)}) + \hat{d}_i^{(0)} \hat{d}_j^{(0)} \right], \quad (14)$$

where \mathbf{R}_{ij} joins the centers of mass of the molecules, $R_{ij} = |\mathbf{R}_{ij}|$, and θ_{ij} is the angle between \mathbf{R}_{ij} and the quantization axis defined by the external dc electric and magnetic fields.

To derive an effective spin-spin interaction Hamiltonian between two $^2\Sigma$ molecules in the effective spin-1/2 states $|\alpha\rangle = |\uparrow\rangle, |\downarrow\rangle$ given by Eq. (13), we project the dipole-dipole interaction (14) onto the two-qubit basis $|\alpha_i\alpha_j\rangle = \{|\uparrow_i\uparrow_j\rangle, |\uparrow_i\downarrow_j\rangle, |\downarrow_i\uparrow_j\rangle, |\downarrow_i\downarrow_j\rangle\}$ to obtain

$$\hat{H}_{\text{dip},ij}^{(q=0)} = \frac{1-3\cos^2\theta_{ij}}{R_{ij}^3} \sum_{\alpha_i,\alpha_j} \sum_{\alpha'_i,\alpha'_j} \langle \alpha_i | d_i^{(0)} | \alpha'_i \rangle \langle \alpha_j | d_j^{(0)} | \alpha'_j \rangle \langle \alpha_i \alpha_j | \alpha'_i \alpha'_j | \quad (15)$$

Evaluating the matrix elements using Eq. (13) and the fact that the operators $\hat{d}_i^{(0)}$ are diagonal in the electron spin quantum number M_S , we arrive at a 4×4 matrix representation of the ED Hamiltonian

$$H_{\text{dip},ij} = \frac{1-3\cos^2\theta_{ij}}{R_{ij}^3} \begin{pmatrix} d_{\uparrow}^2 & 0 & 0 & 0 \\ 0 & d_{\uparrow}d_{\downarrow} & d_{\downarrow}^2 & 0 \\ 0 & d_{\downarrow}^2 & d_{\uparrow}d_{\downarrow} & 0 \\ 0 & 0 & 0 & d_{\downarrow}^2 \end{pmatrix}, \quad (16)$$

Introducing the effective spin-1/2 operators \hat{S}_i^z , \hat{S}_i^+ , and \hat{S}_i^- acting in the two-dimensional Hilbert subspace of the i -th molecule $\{|\downarrow\rangle, |\uparrow\rangle\}$, the ED interaction (16) can be rewritten as a spin-spin interaction Hamiltonian [40]

$$\hat{H}_{\text{dip},ij} = \frac{1-3\cos^2\theta_{ij}}{R_{ij}^3} \left[\frac{J_{\perp}}{2} (\hat{S}_i^+ \hat{S}_j^- + \text{H.c.}) + J_z \hat{S}_i^z \hat{S}_j^z + W_z (\hat{1}_i \hat{S}_j^z + \hat{S}_i^z \hat{1}_j) + V \hat{1}_i \hat{1}_j \right], \quad (17)$$

where $\hat{1}_i$ is the unit operator in the effective two-state space of the i -th molecule, and the spin coupling constants are expressed in terms of the dipole matrix elements [40]

$$\begin{aligned} J_{\perp} &= 2d_{\uparrow\downarrow}^2, & J_z &= (d_{\uparrow} - d_{\downarrow})^2, \\ W_z &= \frac{1}{2}(d_{\uparrow}^2 - d_{\downarrow}^2), & V &= \frac{1}{4}(d_{\uparrow} + d_{\downarrow})^2 \end{aligned} \quad (18)$$

To derive the many-body lattice spin Hamiltonian for interacting $^2\Sigma$ molecules near an ALC, we sum the pairwise interactions given by Eq. (17) over all lattice sites $\hat{H}_{\text{dip}} = \sum_{i,j} \hat{H}_{\text{dip},ij}$ [40]. We further replace the identity operators $\hat{1}_i$ with the total molecular density operator \hat{n}_i , and assume unit filling and homogeneous density of molecules in the lattice, which allows us to neglect the terms proportional to W_z and V in Eq. (17) as constant energy offsets. The resulting spin Hamiltonian for pinned $^2\Sigma$ molecules in a unit-filled lattice takes the form of the XXZ Hamiltonian [see Eq. (3) of the main text]

$$\hat{H}_{\text{dip}} = \sum_{i>j} \left[\frac{J_{ij}^{\perp}}{2} (\hat{S}_i^+ \hat{S}_j^- + \text{H.c.}) + J_{ij}^z \hat{S}_i^z \hat{S}_j^z \right], \quad (19)$$

where $J_{ij}^{\beta} = \frac{1-3\cos^2\theta_{ij}}{R_{ij}^3} J_{\beta}$ ($\beta = ||, \perp$).

Far away from the ALC, the spin exchange coupling constant J_{ij}^{\perp} approaches zero as shown in Fig. 4(d) of the main text, and Eq. (19) reduces to the Ising Hamiltonian [Eq. (1) of the main text]

$$\hat{H}_{\text{dip}} = \sum_{i>j} J_{ij}^z \hat{S}_i^z \hat{S}_j^z. \quad (20)$$

[1] D. DeMille, Quantum computation with trapped polar molecules, *Phys. Rev. Lett.* **88** (2002).

[2] A. André, D. DeMille, J. M. Doyle, M. D. Lukin, S. E. Maxwell, P. Rabl, R. J. Schoelkopf, and P. Zoller, A coherent all-electrical interface between polar molecules and mesoscopic superconducting resonators, *Nat. Phys.* **2**, 636 (2006).

[3] S. F. Yelin, K. Kirby, and R. Côté, Schemes for robust quantum computation with polar molecules, *Phys. Rev. A* **74**, 050301 (2006).

[4] Q. Wei, S. Kais, B. Friedrich, and D. Herschbach, Entanglement of polar symmetric top molecules as candidate qubits, *J. Chem. Phys.* **135**, 154102 (2011).

[5] M. Karra, K. Sharma, B. Friedrich, S. Kais, and D. Herschbach, Prospects for quantum computing with an array of ultracold polar paramagnetic molecules, *J. Chem. Phys.* **144**, 094301 (2016).

[6] K.-K. Ni, T. Rosenband, and D. D. Grimes, Dipolar exchange quantum logic gate with polar molecules, *Chem. Sci.* **9**, 6830 (2018).

[7] P. Yu, L. W. Cheuk, I. Kozyryev, and J. M. Doyle, A scalable quantum computing platform using symmetric-top molecules, *New J. Phys.* **21**, 093049 (2019).

[8] M. L. Wall and L. D. Carr, Emergent timescales in entangled quantum dynamics of ultracold molecules in optical lattices, *New J. Phys.* **11**, 055027 (2009).

[9] L. D. Carr, D. DeMille, R. V. Krems, and J. Ye, Cold and ultracold molecules: science, technology and applications, *New J. Phys.* **11**, 055049 (2009).

[10] A. V. Gorshkov, S. R. Manmana, G. Chen, J. Ye, E. Demler, M. D. Lukin, and A. M. Rey, Tunable superfluidity and quantum magnetism with ultracold polar molecules, *Phys. Rev. Lett.* **107**, 115301 (2011).

[11] A. V. Gorshkov, S. R. Manmana, G. Chen, E. Demler, M. D. Lukin, and A. M. Rey, Quantum magnetism with polar alkali-metal dimers, *Phys. Rev. A* **84**, 033619 (2011).

[12] B. Yan, S. A. Moses, B. Gadway, J. P. Covey, K. R. A. Hazzard, A. M. Rey, D. S. Jin, and J. Ye, Observation of dipolar spin-exchange interactions with lattice-confined polar molecules, *Nature* **501**, 521 (2013).

[13] J. L. Bohn, A. M. Rey, and J. Ye, Cold molecules: Progress in quantum engineering of chemistry and quantum matter, *Science* **357**, 1002 (2017).

[14] N. Y. Yao, M. P. Zaletel, D. M. Stamper-Kurn, and A. Vishwanath, A quantum dipolar spin liquid, *Nat. Phys.* **14**, 405 (2018).

[15] V. V. Albert, J. P. Covey, and J. Preskill, Robust encoding of a qubit in a molecule, *Phys. Rev. X* **10**, 031050 (2020).

[16] A. M. Kaufman and K.-K. Ni, Quantum science with optical tweezer arrays of ultracold atoms and molecules, *Nat. Phys.* **17**, 1324 (2021).

[17] J. Ma, X. Wang, C. P. Sun, and F. Nori, Quantum spin squeezing, *Phys. Rep.* **509**, 89 (2011).

[18] L. Pezzè, A. Smerzi, M. K. Oberthaler, R. Schmied, and P. Treutlein, Quantum metrology with nonclassical states of atomic ensembles, *Rev. Mod. Phys.* **90**, 035005 (2018).

[19] T. Bilitewski, L. De Marco, J.-R. Li, K. Matsuda, W. G. Tobias, G. Valtolina, J. Ye, and A. M. Rey, Dynamical generation of spin squeezing in ultracold dipolar molecules, *Phys. Rev. Lett.* **126**, 113401 (2021).

[20] H. J. Briegel and R. Raussendorf, Persistent entanglement in arrays of interacting particles, *Phys. Rev. Lett.* **86**, 910 (2001).

[21] R. Raussendorf, D. E. Browne, and H. J. Briegel, Measurement-based quantum computation on cluster states, *Phys. Rev. A* **68**, 022312 (2003).

[22] H. J. Briegel, D. E. Browne, W. Dür, R. Raussendorf, and M. Van den Nest, Measurement-based quantum computation, *Nat. Phys.* **5**, 19 (2009).

[23] B. P. Lanyon, P. Jurcevic, M. Zwerger, C. Hempel, E. A. Martinez, W. Dür, H. J. Briegel, R. Blatt, and C. F. Roos, Measurement-based quantum computation with trapped ions, *Phys. Rev. Lett.* **111**, 210501 (2013).

[24] M. Mamaev, R. Blatt, J. Ye, and A. M. Rey, Cluster state generation with spin-orbit coupled fermionic atoms in optical lattices, *Phys. Rev. Lett.* **122**, 160402 (2019).

[25] E. Kuznetsova, T. Bragdon, R. Côté, and S. F. Yelin, Cluster-state generation using van der waals and dipole-dipole interactions in optical lattices, *Phys. Rev. A* **85**, 012328 (2012).

[26] S. Ospelkaus, K.-K. Ni, G. Quéméner, B. Neyenhuis, D. Wang, M. H. G. de Miranda, J. L. Bohn, J. Ye, and D. S. Jin, Controlling the hyperfine state of rovibronic ground-state polar molecules, *Phys. Rev. Lett.* **104**, 030402 (2010).

[27] J. A. Blackmore, P. D. Gregory, S. L. Bromley, and S. L. Cornish, Coherent manipulation of the internal state of ultracold ^{87}Rb - ^{133}Cs molecules with multiple microwave fields, *Phys. Chem. Chem. Phys.* **22**, 27529 (2020).

[28] S. Kotochigova and D. DeMille, Electric-field-dependent dynamic polarizability and state-insensitive conditions for optical trapping of diatomic polar molecules, *Phys. Rev. A* **82**, 063421 (2010).

[29] L. Caldwell, H. J. Williams, N. J. Fitch, J. Aldegunde, J. M. Hutson, B. E. Sauer, and M. R. Tarbutt, Long rotational coherence times of molecules in a magnetic trap, *Phys. Rev. Lett.* **124**, 063001 (2020).

[30] S. Burchesky, L. Anderegg, Y. Bao, S. S. Yu, E. Chae, W. Ketterle, K.-K. Ni, and J. M. Doyle, Rotational coherence times of polar molecules in optical tweezers, *Phys. Rev. Lett.* **127**, 123202 (2021).

[31] A. L. Collopy, M. T. Hummon, M. Yeo, B. Yan, and J. Ye, Prospects for a narrow line MOT in YO, *New J. Phys.* **17**, 055008 (2015).

[32] A. L. Collopy, S. Ding, Y. Wu, I. A. Finneran, L. Anderegg, B. L. Augenbraun, J. M. Doyle, and J. Ye, 3D magneto-optical trap of yttrium monoxide, *Phys. Rev. Lett.* **121**, 213201 (2018).

- [33] S. Ding, Y. Wu, I. A. Finneran, J. J. Burau, and J. Ye, Sub-doppler cooling and compressed trapping of YO molecules at μ K temperatures, *Phys. Rev. X* **10**, 021049 (2020).
- [34] Y. Wu, J. J. Burau, K. Mehling, J. Ye, and S. Ding, High phase-space density of laser-cooled molecules in an optical lattice, *Phys. Rev. Lett.* **127**, 263201 (2021).
- [35] S. Truppe, H. J. Williams, M. Hambach, L. Caldwell, N. J. Fitch, E. A. Hinds, B. E. Sauer, and M. R. Tarbutt, Molecules cooled below the doppler limit, *Nat. Phys.* **13**, 1173 (2017).
- [36] L. Anderegg, B. L. Augenbraun, Y. Bao, S. Burchesky, L. W. Cheuk, W. Ketterle, and J. M. Doyle, Laser cooling of optically trapped molecules, *Nat. Phys.* **14**, 890 (2018).
- [37] J. F. Barry, D. J. McCarron, E. B. Norrgard, M. H. Steinecker, and D. DeMille, Magneto-optical trapping of a diatomic molecule, *Nature (London)* **512**, 286 (2014).
- [38] D. J. McCarron, M. H. Steinecker, Y. Zhu, and D. DeMille, Magnetic trapping of an ultracold gas of polar molecules, *Phys. Rev. Lett.* **121**, 013202 (2018).
- [39] J. Aldegunde, B. A. Rivington, P. S. Źuchowski, and J. M. Hutson, Hyperfine energy levels of alkali-metal dimers: Ground-state polar molecules in electric and magnetic fields, *Phys. Rev. A* **78**, 033434 (2008).
- [40] M. L. Wall, K. R. A. Hazzard, and A. M. Rey, Quantum magnetism with ultracold molecules, in *From Atomic to Mesoscale. The Role of Quantum Coherence in Systems of Various Complexities* (World Scientific, 2015) pp. 3–37.
- [41] See Supplemental Material at [URL] for additional information about molecular Hamiltonians and interactions used in this work, and for the derivation of effective spin-spin interactions.
- [42] F. Herrera, Y. Cao, S. Kais, and K. B. Whaley, Infrared-dressed entanglement of cold open-shell polar molecules for universal matchgate quantum computing, *New J. Phys.* **16**, 075001 (2014).
- [43] J. W. Park, Z. Z. Yan, H. Loh, S. A. Will, and M. W. Zwierlein, Second-scale nuclear spin coherence time of ultracold $^{23}\text{Na}^{40}\text{K}$ molecules, *Science* **357**, 372 (2017).
- [44] J.-Y. Zhang, Z.-W. Zhou, and G.-C. Guo, Eliminating next-nearest-neighbor interactions in the preparation of cluster state, *Chin. Phys. Lett.* **28**, 050301 (2011).
- [45] P. D. Gregory, J. A. Blackmore, S. L. Bromley, J. M. Hutson, and S. L. Cornish, Robust storage qubits in ultracold polar molecules, *Nat. Phys.* **17**, 1149 (2021).
- [46] B. Friedrich and D. Herschbach, Steric proficiency of polar $^2\Sigma$ molecules in congruent electric and magnetic fields, *Phys. Chem. Chem. Phys.* **2**, 419 (2000).
- [47] T. V. Tscherbul and R. V. Krems, Controlling electronic spin relaxation of cold molecules with electric fields, *Phys. Rev. Lett.* **97**, 083201 (2006).
- [48] E. Abrahamsson, T. V. Tscherbul, and R. V. Krems, Inelastic collisions of cold polar molecules in nonparallel electric and magnetic fields, *J. Chem. Phys.* **127**, 044302 (2007).
- [49] M. A. Perlin, C. Qu, and A. M. Rey, Spin squeezing with short-range spin-exchange interactions, *Phys. Rev. Lett.* **125**, 223401 (2020).
- [50] E. Altuntaş, J. Ammon, S. B. Cahn, and D. DeMille, Demonstration of a sensitive method to measure nuclear-spin-dependent parity violation, *Phys. Rev. Lett.* **120**, 142501 (2018).
- [51] T. V. Tscherbul, J. Ye, and A. M. Rey, State-insensitive trapping conditions for microwave-dressed rotational states of polar molecules, in preparation (2022).
- [52] J. Aldegunde, H. Ran, and J. M. Hutson, Manipulating ultracold polar molecules with microwave radiation: The influence of hyperfine structure, *Phys. Rev. A* **80**, 043410 (2009).
- [53] J. Brown and A. Carrington, *Rotational Spectroscopy of Diatomic Molecules* (Cambridge University Press, 2003).
- [54] T. V. Tscherbul, J. Kłos, L. Rajchel, and R. V. Krems, Fine and hyperfine interactions in cold YbF-He collisions in electromagnetic fields, *Phys. Rev. A* **75**, 033416 (2007).